THERMAL-MASS EXCHANGE IN A POLYMERIZING LIQUID WITHIN A CYLINDRICAL RESERVOIR

Z. P. Shul'man, B. M. Khusid, V. B. Érenburg, É. V. Ivashkevich, I. L. Ryklina, and N. O. Vlasenko

UDC 541.64

The nonisothermal kinetics of polymerization in nonmoving inhomogeneous systems are studied numerically.

The development of a new technology — chemical forming, which simultaneously combines production of material and the part made of that material, has stimulated the need to study features of the thermal-mass transport process in a polymer composition during mixture solidification in the forechamber and the completion of that solidification within a form. The character of such processes has a dominating effect on not only the technological parameters but the quality of the material and part and its ultimate performance in use. Because of the high heat of the solidification reaction (up to 500 kJ/g) these processes are significantly nonisothermal. The conditions created for heat exchange have a significant effect upon the evolution in time of the temperature and solidification fields, their spatial inhomogeneity, and consequently, the inhomogeneous microstructure of the product and its mechanical, thermal, and other properties.

We will study nonisothermal solidification of a nonmoving inhomogeneous medium (epoxy resin with amine hardener). We describe solidification kinetics by a macrokinetic model [1], in which reactions of primary and secondary amines occur with epoxy groups and epoxy—alcohol complexes with formation of alcohol groups and tertiary amines. With consideration of material balance the corresponding kinetic relationships have the form

$$\frac{dY}{dt} = k_1 A_1 \mathrm{E}(Y) + k_1' A_1 k_\mathrm{p} C(Y)\,\mathrm{E}(Y) + k_2' A_2 k_\mathrm{p} C(Y)\,\mathrm{E}(Y);$$
$$\frac{dA_1}{dt} = -k_1 A_1 \mathrm{E}(Y) - k_1' A_1 k_\mathrm{p} C(Y)\,\mathrm{E}(Y), \tag{1}$$

where

$$\mathrm{E}(Y) = \frac{1}{2}[\mathrm{E}_0 - C_0 - 2Y - k_\mathrm{p}^{-1}] + \sqrt{(2Y - \mathrm{E}_0 + C_0 + k_\mathrm{p}^{-1})^2 + 4(-Y + \mathrm{E}_0)k_\mathrm{p}^{-1}};$$
$$C(Y) = [\mathrm{E}_0 - C_0 - \mathrm{E}(Y)]/[1 + 2k_\mathrm{p}\mathrm{E}(Y)],$$

$Y = E_0 - E - (EA)$ is the number of epoxy groups, $A_2 = Y - 2A_3$; $A_3 = A_1 + Y - A_{10}$; $(EA) = k_e EA$; reaction rates depend on temperature by an Arrhenius law $k_1 = k_{10}\exp(-E_1/RT)$, $k_1' = k_{10}'\exp(-E_1/RT)$; $k_2' = k_{20}'\exp(-E_2'/RT)$, from thermodynamic considerations the equilibrium constant $k_e = \exp((\Delta S/R) - (\Delta H/RT))$. Heat liberation intensity is determined by the rate of change of conversion depth $\Phi = Q_{E0}(\partial\beta_1/\partial T)$, $\beta_1 = Y/E_0$. At the initial moment $A = A_{10}$, $E = E_0$, $A_0 = Y = C = 0$.

A. V. Lykov Heat and Mass Transport Institute, Academy of Sciences of the Belorussian SSR, Minsk.
Translated from Inzhenerno-Fizicheskii Zhurnal, Vol. 60, No. 1, pp. 51-60, January, 1991. Original article submitted December 11, 1989.

0022-0841/91/6001-0043$12.50

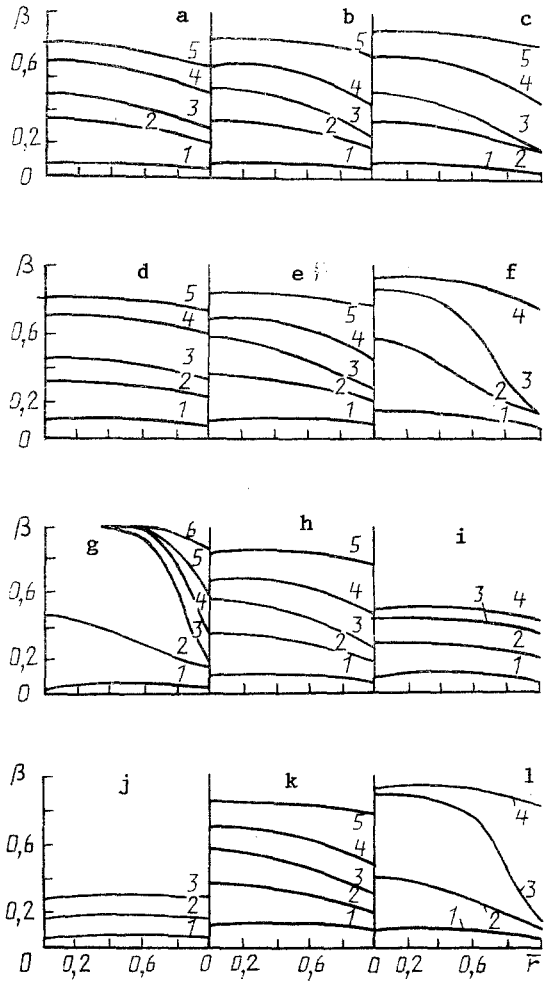

Fig. 1. Effect of initial temperature (a-c), reservoir geometry (d-f), reagent ratio (g-i), and initial epoxy group concentration (j-l) on evolution of spatial inhomogeneity of degree of conversion fields: a) T = 60°C, 1, t = 37.5 min; 2, 82.5; 3, 97.5; 4, 135.5; 5, 180; b) T = 65°C, 1, t = 30 min; 2, 60; 3, 75.5; 4, 77.5; 5, 180; c) T = 70°C, 1, t = 22.5 min; 2, 45; 3, 52.5; 4, 82.5; 5, 180; d) $R_0 = 7 \cdot 10^{-3}$ m, 1, t = 30 min; 2, 67.5; 3, 82.5; 4, 127.5; 5, 180; e) $R_0 = 10 \cdot 10^{-3}$ m, 1, t = 30 min; 2, 60; 3, 72.5; 4, 77.5; 5, 180, f) $R_0 = 15 \cdot 10^{-3}$ m, 1, t = 30 min; 2, 45; 3, 52.5; 4, 180; g) $B = 5 \cdot 10^3$ mol/m^3, 1, t = 7.5 min; 2, 22.5; 3, 30; 4, 37.5; 5, 52.5; 6, 82.5; h) B = 0, 1, t = 30 min; 2, 60; 3, 75; 4, 77.5; 5, 180; i) $B = -2.10^3$ mol/m^3, 1, t = 52.5 min; 2, 112; 3, 157.5; 4, 180; j) $E = 2 \cdot 10^3$ mol/m^3, 1, t = 52.5 min; 2, 127.5; 3, 180; k) $E = 5 \cdot 10^3$ mol/m^3, 1, t = 30 min; 2, 60; 3, 75; 4, 127.5; 5, 180; l) $E = 7 \cdot 10^3$ mol/m^3, 1, t = 15 min; 2, 30; 3, 137.5; 4, 180.

Analysis of the phase portrait of system (1) has shown [2] that the macrokinetic model properly reflects the features of solidification kinetics: the final composition of the material corresponds to a stable rest point. The phase portrait depends upon the degree of nonstoichiometry $B = 2A_{10} - E_0$. Variation of the catalytic reaction rates k'_1, k'_2, and the initial epoxy group concentration produces various changes in composition with time: for $k'_2 < k'_1$ the reaction is completed due to secondary amines, while for $k'_2 > k'_1$ its completion depends upon the quantity E_0. For $E_0 \lesssim E_{cr} = k_1/k_p(k'_2 - k'_1)$ the reaction is again completed solely because of secondary amines, while at $E_0 > E_{cr}$ conversion of primary amines into secondary continues over the course of the entire reaction.

Analysis of the limiting cases of isothermal and adiabatic solidification [2] shows that due to the intense nonlinearity of the kinetic equations only numerical study is possible. Consideration of spatial inhomogeneity of the temperature fields and degree of conversion in real chemical reactors complicates the problem even more.

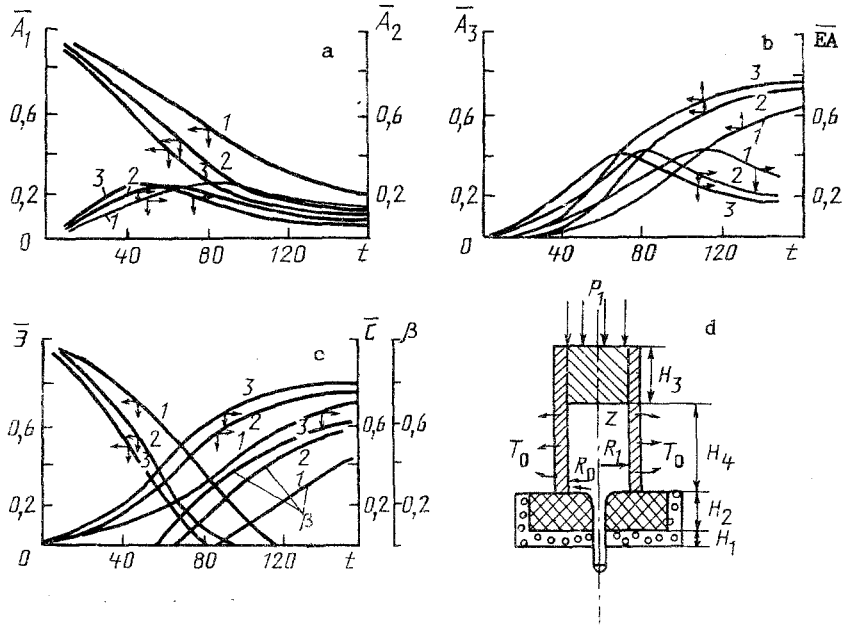

Fig. 2. Change with time in relative expenditure of primary and secondary amines (a), relative expenditure of tertiary amines and relative concentration of epoxy–alcohol complexes (b), relative expenditure of epoxy groups, relative concentration of alcohol groups and degree of conversion (c) in experimental apparatus, and diagram of apparatus (d): 1) T = 60°C; 2) 65; 3) 67.5. t, min.

We will consider nonisothermal solidification of a nonmoving reacting system located in a cylindrical reservoir (reactors). Neglecting natural convection, the mathematical formulation of the problem includes the thermal conductivity equation and a relationship for the structure parameters [3, 4]:

$$\rho c \frac{\partial T}{\partial t} = \operatorname{div}(\lambda \nabla T) + \Phi(\beta, T), \tag{2}$$

$$\frac{\partial \beta}{\partial t} = f(\beta, T), \tag{3}$$

where

$$\Phi = \begin{cases} Q\vartheta_0 \dfrac{\partial \beta_1}{\partial t}, & \mathbf{x} \in \Omega_0, \\ 0, & \mathbf{x} \in \Omega_1; \end{cases}$$

ρ, c, λ are functions piecewise continuous along the spatial variables. As is Q, they are independent of temperature and the structural parameters of the reacting medium.

For the kinetics we will use macrokinetic system (1). The structure parameter vector has seven components: $\beta_1 = Y/E_0$; $\beta_j = A_{j-1}/A_{10}$ (j = 2, 3, 4); $\beta_5 = E/E_0$, $\beta_6 = C/E_0$, $\beta_7 = (EA)/E_0$. For any kinetic model system (2), (3) is quasilinear and bound by nonlinear right sides.

We will limit ourselves to the case of axial symmetry. We introduce the dimensionless variables $R = R_0\bar{r}$, $Z = R_0\bar{z}$, $T = T_0\tau$, $T - T_0 = (T_* - T_0)\theta$.

In these variables Eqs. (2), (3) take on the form:

$$d \frac{1}{\mathrm{Fo}} \frac{\partial \theta}{\partial \tau} = \frac{1}{\bar{r}} \frac{\partial}{\partial \bar{r}} e\bar{r} \frac{\partial \theta}{\partial \bar{r}} + \frac{\partial}{\partial \bar{z}} \lambda e \frac{\partial \theta}{\partial \bar{z}} + \bar{\Phi}(\beta, \theta); \tag{4}$$

$$\frac{\partial \beta}{\partial \tau} = \zeta \varphi(\beta, \theta), \tag{5}$$

TABLE 1. Thermophysical Properties of Wall Materials and Resin

Material	λ, w/(m·K)	ρ·10⁻³, kg/m³	c, kJ/(kg·K)
ED-20	0,153	1,14	1,56
Caprolon	0,16	1,13	1,7
Teflon	0,209	2,15	1,17
Ebonite	0,163	1,15	1,43
Plastic foam	0,034	0,1	0,25

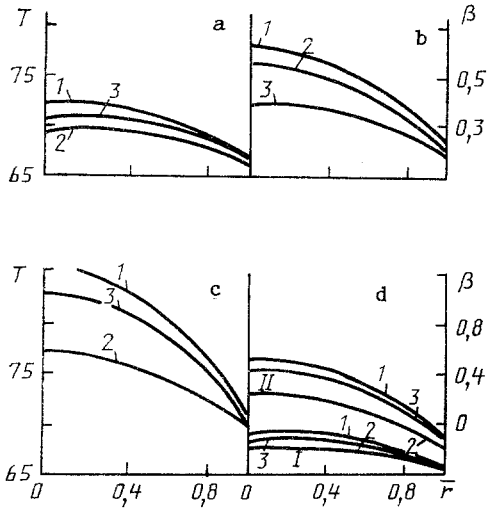

Fig. 3

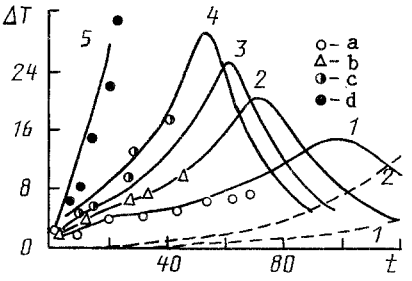

Fig. 4

Fig. 3. Development over time of spatial inhomogeneity in temperature and conversion fields in solidifying composition over radius and reservoir height for initial polymerization process temperature T = 65°C: a) t = 30 min; b) 52.5; c) 75; d) 90 (I), 120 (II): 1) center of reservoir; 2) top; 3) 1/4 form center upward. T, °C.

Fig. 4. Heating of solidifying composition at various initial polymerization process temperatures. Solid curves) calculation by macrokinetic model: 1) T = 60°C; 2) 65; 3) 67.5; 4) 70; 5) 80. Experimental data: a) T = 60°C; b) 65; c) 70; d) 80. Dashes) phenomenological model: 1) T = 60°C; 2) 65. T, °C.

where

$$\varphi_2(\bar{\beta}_1, \bar{\beta}_2, \theta) \equiv \varphi_2(\bar{Y}, A_1, \theta) = -A_1\left[\exp\left(\frac{E_1}{RT_0}\frac{\theta}{\theta+\theta_*}\right)\bar{E}(\bar{Y}) + \right.$$

$$\left. + \frac{k'_{10}}{k_{10}}\exp\left(\frac{E_1-E'_1}{RT_0}\right)\exp\left(\frac{E'_1}{RT_0}\frac{\theta}{\theta+\theta_*}\right)(1-\bar{Y}-\bar{E}(\bar{Y}))\right],$$

$$\varphi_1(\bar{\beta}_1, \bar{\beta}_2, \theta) \equiv \varphi_1(\bar{Y}_1, A_1, \theta) = -\varphi_2(\bar{Y}, A_1, \theta) + \psi_2(\bar{Y}, \bar{A}_1, \theta),$$

$$\psi_2(\bar{Y}, \bar{A}_1, \theta) = 2\left(1 - A_1 - \frac{E_0}{2A_{10}}\bar{Y}\right)(1-\bar{Y}-E(\bar{Y}))\frac{k'_{20}}{k_{10}} \times$$

$$\times \exp\left(\frac{E_1-E'_2}{RT_0}\right)\exp\left(\frac{E'_2}{RT_0}\frac{\theta}{\theta+\theta_*}\right); \quad \bar{\Phi} = \Phi St_0/(QE_0);$$

$$k_0 = k_{10}\exp\left(-\frac{E_1}{RT_0}\right); \quad \bar{E}(\bar{Y}) = \frac{1}{2}[-(2\bar{Y}-1+(k_pE_0)^{-1}) +$$

$$+\sqrt{(2\bar{Y}-1+(k_pE_0)^{-1})^2+4(1-\bar{Y})(k_pE_0)^{-1}}];$$

$$k_p = k_{p0} \exp\left(-\frac{\Delta H}{RT_0}\,\frac{\theta_*}{\theta+\theta_*}\right),\ \theta_* = T_0/(T_* - T_0),\ \ k_{p0} = \exp\left(\frac{\Delta S}{R}\right).$$

Here and below $\bar{Y}_E$, $\bar{E}$, $\bar{C}$, $(\bar{E}\bar{C})$ are dimensionless forms of the corresponding variables without the bar, referenced to E_0, $\bar{A}_i = A_i/A_{10}$, $i = 1, 2, 3$.

The problem has the following dimensionless parameters:

$$\mathrm{Fo} = \frac{\lambda_1}{\rho_1 c_1}\,\frac{t_0}{R_0^2},\quad S = \frac{E_0 Q R_0^2}{\lambda_1 t_0 (T_* - T_0)},\quad d = \frac{\rho c}{\rho_1 c_1},\quad e = \frac{\lambda}{\lambda_1},$$

$$\zeta = t_0 k_0 E_0,\quad \Gamma = \frac{H}{R},$$

where the subscript 1 refers to parameters of the reaction medium. In connection with specification of various heat exchange conditions with the external medium on the reservoir surface additional parameters may appear, for example, the dimensionless temperature of the external medium, Biot and Rayleigh numbers, etc.

Below we will analyze the following three important regimes for nonsteady and inhomogeneous temperature fields:

1) solidification duration significantly exceeds the time for diffusion propagation of heat in the reservoir, $t_{sol} \gg R_0^2/a$, i.e., solidification occurs under conditions close to isothermal;

2) constrained regime: $t_{sol} \ll R_0^2/a$ — the heat cannot be removed, and solidification takes place under conditions close to adiabatic;

3) solidification and diffusion times are of the same order; the reaction occurs in a significantly nonsteady inhomogeneous temperature field.

The limiting cases of isothermal and purely adiabatic solidification were considered in [2].

We will consider the realization of these regimes as a function of solidification temperature, reservoir geometry, heat exchange conditions with the external medium, kinetic parameters of the reaction medium, initial concentrations of the reaction groups and hardening agent ($\bar{B} = 1 - E_0/2A_{10}$, $\bar{B} = 0$ being stoichiometry, $\bar{B} < 0$, insufficient hardener, $\bar{B} > 0$, excess hardener).

To obtain a numerical solution of Eqs. (2), (3) we use the method of splitting into physical and chemical factors, as well as splitting by directions.

We will consider two splitting techniques:

Ia) chemical conversions under adiabatic conditions;

Ib) diffusion heat redistribution in accordance with external conditions;

IIa) chemical conversions under nonisothermal conditions;

IIb) heat exchange with sources distributed over the volume, liberating heat during the chemical conversion stage.

The first splitting scheme requires solution of a system of nonlinear ordinary differential equations for the kinetic parameters in the first semistep and solution of the linear problem for the thermal conductivity equation in the second semistep. The second scheme also involves solution of the system in the first semistep, but requires solution of a quasilinear thermal conductivity equation in the second, which is related to the necessity of iteration. Calculations of heat exchange and solidification kinetics available in the literature [5-7] were performed by scheme II. We will consider both methods and show that the use of scheme I will reduce required computer time by a factor of approximately two times for the same computation accuracy.

A fourth-order accuracy Runge—Kutta method was used for numerical solution of the kinetic equations. The solution of the initial-boundary problem for the thermal conductivity equation with discontinuous coefficients was sought by a finite difference method. A homogeneous monotonic conservative difference scheme on a nonuniform grid with order of approximation $O(\tau + h^2)$ was obtained by the interpolation method [8, 2]. The numerical algorithm for solution of the difference equations was constructed by splitting over coordinate and realized by two successive drives. The technique was absolutely stable.

System (4), (5) is solved numerically in the following order. Following splitting scheme I, the Runge—Kutta method is used to solve the equation for the solidification parameters, in which $\theta = \bar{\theta}^n = \theta^n + \mathrm{Fo}S(\beta_1 - \beta_1^n)$. As a result we find β^{n+1}. Then, taking $\theta^n = \bar{\theta}^n$, from the difference analog of the split equation (4) at $\bar{\Theta} = 0$ we find θ^{n+1}. The computation process is then repeated.

When splitting scheme II is used, after finding β^{n+1} from the kinetic equation at $\theta = \theta^n = \text{const}$ we calculate the power of volume heat sources $\bar{\Phi}(\beta^{n+1}, \theta) = S\xi\varphi(\beta^{n+1}, \theta)$ in the region $(\bar{r}, \bar{z}) \in \Omega_0$. The system of difference equations corresponding to Eq. (4) is linear on the right side in the function θ_{ij}^{n+1}. A solution is found by the iteration method. The iteration procedure is constructed with the following linearization:

$$\theta_{ij}^{n+1} \to \overset{\nu+1}{\theta}{}^{n+1}, \ \bar{\Phi}_{ij}^{n+1}(\beta^{n+1}, \ \theta^{n+1}) \to \Phi_{ij}^{n+1}(\beta^{n+1}, \ \overset{\nu}{\theta}{}^{n+1}),$$

where $\overset{\nu}{\theta}{}^{n+1}$ is the value of the ν-th iteration of the dimensionless temperature. For the initial iteration we take the value of the function $\overset{0}{\theta}_{ij}$ in the preceding time layer $\overset{0}{\theta}_{ij}{}^{n+1} = \theta_{ij}{}^{n}$. The difference scheme is linear in $\overset{\nu+1}{\theta}{}^{n+1}$. Successive calculation of iterations is terminated when the condition $|\overset{\nu+1}{\theta}_{ij}{}^{n+1} - \overset{\nu}{\theta}_{ij}{}^{n+1}| \leq \varepsilon$ is satisfied, ε being the specified accuracy. With simple alternation of directions we first solve the first of the difference equations corresponding to Eq. (4), then use $\overset{\nu+1}{\theta}{}^{n+\frac{1}{2}}$ to solve the second equation for $\overset{\nu+1}{\theta}{}^{n+1}$. The equation thus obtained is used as an iteration to calculate new values of the function $\bar{\Phi}_{ij}{}^{n+1}$ and the cycle is repeated.

To provide the required accuracy the time step is chosen of the order of magnitude of the square of the step in spatial variables $St_{n+1} \lesssim h^2$ (the "chemical" step is not limited since the order of approximation there is $O(\tau^4)$). The intensity of internal heat liberation sources determined by the parameters of the reacting medium changes during the course of solidification, passing through a maximum. To reduce computer time, we correspondingly increase or reduce the time step. Each time Runge's rule serves as the criterion of suitability of the step size chosen.

The value of T_* figuring in determination of the dimensionless temperature is determined from the condition $0.2 \lesssim \text{Fo}S \lesssim 8$, whence for the majority of calculations performed $T_* \simeq 1.2\, T_0$.

A series of methodological calculations was performed with the gaol of testing the possibilities of the proposed algorithm. The algorithm constructed for calculating temperature fields was tested with a series of linear problems having analytical solutions. Also tested were the conservative nature of the difference scheme and the effect of the splitting schemes I and II on results obtained for kinetics and heat exchange in spatially inhomogeneous systems.

Good agreement was obtained with thermal balance over the reservoir volume. The divergence did not exceed $5 \cdot 10^{-2}$%. It was established that the order of solving the equations in system (4), (5) for $St_{n+1} \sim (\Delta\bar{r})^2$ had practically no effect on the numerical modeling results, i.e., alternation of drive directions opposite the normal is not required.

In a number of problems with types I, II, III, and mixed heat exchange conditions the effect of the splitting method on results was studied. Comparison revealed that results with both methods practically coincided. Since, for example, to obtain an accuracy $\varepsilon = 5 \cdot 10^{-4}$ from three to six temperature iterations are required for each time step, the computer time for calculating the heat exchange and solidification kinetics with scheme II is almost twice as great as for scheme I. Numerous calculations of nonlinear problems on a sequence of ever denser grids showed the good convergence of the numerical solutions.

Thus, the calculation algorithm described above based on splitting scheme I can be recommended for the class of heat exchange and solidification kinetics problems under consideration.

This algorithm can be used to solve a wide class of problems with various types of heat exchange conditions on the external surface of the reservoir containing the reacting medium. The reservoir itself may have thick walls, consisting of materials with differing thermophysical properties. We will begin our analysis of conversions in a liquid uncomplicated by transport processes in the walls with the case of thermally thin walls.

We will consider solidification of ED-20 resin with metaphenylendiamine hardener in a cylindrical vessel $H = 19.5 \cdot 10^{-3}$ m high with thermally insulated ends and temperature stabilized lateral surface ($T_1 = T_0 = \text{const}$). The thermophysical, kinetic, and thermodynamic parameters of the system are taken from [1, 9, 10]:

$\rho = 1.14 \cdot 10^3$ kg/m, $c_p = 1.56$ kJ/(kg·deg), $\lambda = 0.153$ W/(m·deg), $Q = 1.09 \cdot 10^2$ kJ/mol, $k_{10} = 2$ m^3/(mol·sec), $k'_{10} = 0.125$ m^3/(mol·sec), $k'_{20} = 0.55$ m^3/(mol·sec), $E_1 = 52.3$ kJ/mol, $E'_1 = 39.4$ kJ/mol, $E'_2 = 41.06$ kJ/mol, $k_{e0} = \exp(\Delta S/R) = 0.144 \cdot 10^{-5}$ m^3/mol, $\Delta H = -19.27$ kJ/mol, $E_e = 6 \cdot 10^3$ mol/m^3, $A_{10} = 2.5 \cdot 10^3$ mol/m^3 (stoichiometric ratio).

Figure 1 shows calculation results reflecting the effect of initial temperature T_0, reservoir geometry, reagent ratio, and initial epoxy group concentration on evolution of the degree of conversion β. Increase in T_0 significantly accelerates the solidification process and intensifies the nonuniformity of the β distribution over radius, especially at the moment of maximum heating of the center of the volume relative to the wall. The effect of reservoir dimensions,

and thus, indirectly, heat removal conditions, manifests itself analogously. Retarding the diffusion distribution of heat (Fig. 1d-f) leads to more intense heating of the medium, especially in the center of the reservoir. We then see not only an increase in β, but the degree of nonuniformity of the latter's distribution over radius. An excess of amines encourages rapid occurrence of the solidification reaction, while their shortage retards it significantly (Fig. 1g-i). Thus, for one and the same time (t = 52.5 min) for change in B from $5 \cdot 10^3$ to $-2 \cdot 10^3$ mol/m^3 β increases by a factor of ten. The ratio $\beta_{center}/\beta_{wall}$, i.e., nonuniformity of E_0 within the volume, also increases significantly (factor of three times). Increase in E_0 encourages rapid reaction, an excess of epoxy groups aiding full interaction with the reactive hardener groups (Fig. 1j-l).

As an example of solidification in a reservoir with thick walls we will consider results of a calculation for an experimental apparatus used for study of thermal processes in polymerization of solidifying compositions (Fig. 2). The geometric characteristics of the device were as follows: $R_0 = 11.55 \cdot 10^{-3}$ m, $R_1 = 9.25 \cdot 10^{-3}$ m, $H_1 = 3.5 \cdot 10^{-3}$ m, $H_2 = 11 \cdot 10^{-3}$ m, $H_3 = 21 \cdot 10^{-3}$, $H_4 = 19.5 \cdot 10^{-3}$ m.

The thermophysical properties of the wall materials and ED-20 resin are presented in Table 1.

Numerical calculations were performed both with consideration of heat loss due to free convection [2], and for the case of thermally insulating faces. These calculations showed that change in thermal conditions on the face surfaces has practically no effect on the temperature to which the volume center is heated, T_{max}, the mean volume degree of conversion β_{cp} m, and the mean temperature T_m. Thus, for T_0 = 60°C the maximum deviation comprises 0.4% for T_{max} and T_m, and 1% for β_{cp}m, while for T_0 = 67.5°C the corresponding values are 0.5 and 1.4%, respectively. Thus, the face surfaces of the real device can be considered adiabatic.

The numerical modeling of the solidification process in the apparatus provided the kinetics of change in model structural parameters, and the mean volume characteristics, together with their changes over time and with temperature. For Fig. 2 we can determine the relative concentration of any structural components of the system for any moment in time for various initial temperatures. A higher initial temperature encourages more rapid increase (β, A_2, A_3, EA, A) or decrease (A_1, E) in all kinetic parameters.

As was noted above, to obtain a product with a homogeneous microstructure it is necessary to carry out the solidification process such that the inhomogeneity in temperature and conversion fields are at a minimum. Numerical modeling of the evolution of these fields was carried out for reservoir wall stabilization at temperatures 60°C < T_0 < 80°C. Figure 3 shows corresponding characteristic profiles for T_0 = 65°C. It was found that heating encourages intensification of spatial inhomogeneity in the temperature and degree of conversion fields. Thus, at T_0 = 60°C the temperature difference between the center and top of the reservoir (ΔT_h), as well as the difference between center and wall (ΔT_r) comprised 6 and 11°C for 97.5 min, with degree of solidification 0.1 and 0.12 respectively. For comparison, we will note that at T_0 = 80°C these differences comprise (at 26.2 min) 30 and 45°C, 0.25 and 0.4. This principle prevailed in all temperature regimes studied. With increase in T_0 the time at which the greatest field inhomogeneity was reached decreased significantly. At T_0 = 60°C it comprised 97.5 min, for 65°C, 75 min, for 67.5°C, 60 min, and for 80°C, 26.2 min, with the maximum temperature nonuniformity corresponding to the greatest nonuniformity in the degree of conversion field. The general principle governing evolution of the temperature and degree of conversion fields in all regimes is that spatial inhomogeneity first intensifies with increase in heating, then decreases. Thus, the theoretical calculation performed permits determination of not only the optimum temperatures, but optimum time regimes for solidification.

Calculation of the Kamal phenomenological model [11] were also performed. Results were compared to the two kinetic models using data of specially conducted experiments. Heating values at the center of a "thick-wall" reservoir (with geometric parameters and thermophysical properties corresponding to the calculations) were compared. Results are presented in Fig. 4. As is evident from the figure, calculations with the macroscopic model agree well with measurements, especially at lower initial temperatures. Some elevation of the theoretical values as compared to experiment for higher lateral surface temperatures ($T_{stab} = T_0$) can be explained by a possible slight shift of the thermocouple from the center of the volume. With increase in T_0 the nonuniformity of the temperature distribution over the volume increases intensely, as was shown above, therefore the uncertainty of thermocouple indications due to possible displacement naturally increases.

Comparison of the two approaches to description of solidification kinetics with experimental data permits the conclusion of good agreement of calculations by the macrokinetic model with the real process. The phenomenological model predicts reduced kinetic characteristics and slowing of their rates of change. Since many material characteristics of both models were taken from the literature, it can be suggested that the composite parameter β in the

phenomenological approach ignores certain significant features of the real kinetics and initial reagents. Therefore in contrast to the macrokinetic model with a phenomenological approach it is necessary to determine corresponding model parameters (constants) for every system studied.

Thus, the nonisothermal kinetics of polymerization of nonmoving inhomogeneous systems have been studied using the proposed calculation method. Results of calculations by the macrokinetic model of solidification of an epoxy resin by amine type hardeners agree with experimental data. Knowing the effect on the process of various parameters, one can choose regimes optimal with respect to temperature, reagent ratio, initial concentration, and reservoir geometry to provide homogeneity of the material produced.

NOTATION

Here A_1, A_2, A_3, E, A, (EA) are primary, secondary, tertiary amine, epoxy group, alcohol group, epoxy-alcohol complex concentrations; T, temperature; E_0, A_{10}, C_0, initial concentrations of epoxy groups, primary amines, and alcohol groups; ΔS, change in entropy: ΔH, change in enthalpy; E_1, E'_1, E'_2, activation energies; R, universal gas constant; Q, thermal effect of reaction; Θ, power of internal chemical heat sources; β = colon(β_1, ..., β_n), structure parameter vector; $\beta = \beta_1$, conversion depth; R_0, reservoir radius; ρ, c, λ, thermophysical characteristics of reacting medium and vessel walls; t_0, time scale; T_0, T_1, initial temperature and temperature of thermally stabilized reservoir side wall; T_*, temperature scale; r, z, cylindrical coordinates; Ω_0, Ω_1, regions occupied by reactive medium and reservoir walls respectively; t, time; a, thermal diffusivity coefficient.

LITERATURE CITED

1. Kh. A. Arutyunyan, S. P. Davtyan, B. A. Rozenberg, and N. S. Enikolopyan, Vysokomol. Soedin., **16(A)**, No. 9, 2115-2122 (1974).
2. Z. P. Shul'man, B. M. Khusid, I. L. Rykina, et al., Thermal Processes and Conversion Kinetics in Solidification of Oligomer Compositions, Preprint ITMO Akad. Nauk Beloruss. SSR, No. 5 [in Russian], Minsk (1988).
3. Z. P. Shul'man, B. M. Khusid, I. L. Ryklina, et al., Dokl. Akad. Nauk SSSR, **305**, No. 6, 1420-1424 (1989).
4. Z. P. Shul'man, S. P. Davtyan, B. M. Khusid, et al., Reports to the Minsk International Forum, May 24-27, 1988 [in Russian], Minsk (1988), pp. 16-17.
5. S. A. Bostandzhiyan, A. G. Merzhanov, and N. M. Pruchkina, Zh. Prikl. Mekh. Tekh. Fiz., No. 5, 38-43 (1968).
6. S. A. Bostandzhiyan, V. I. Boyarchenko, P. V. Zhirkov, and Zh. A. Zinenko, Zh. Prikl. Mekh. Tekh. Fiz., No. 1, 130-137 (1979).
7. A. M. Girshin and V. B. Nemirovskii, Zh. Prikl. Mekh. Tekh. Fiz., No. 1, 72-81 (1983).
8. A. A. Samarskii, Introduction to the Theory of Difference Systems [in Russian], Moscow (1982).
9. Kh. A. Arutyunyan, S. P. Davtyan, B. A. Rozenberg, and N. S. Enikolopyna, VMS, **17(A)**, No. 3, 389-395 (1975).
10. Z. P. Shul'man, B. M. Khusid, I. L. Ryklina, et al., Reports to the Belorussian Scientific-Technical Conference "Thermal Analysis for Intensification of Technological Processes and Development of Progressive Materials" [in Russian], Minsk (1988), p. 122.
11. S. Sourour and M. R. Kamal, Thermochim. Acta, **14**, 41-59 (1976).